Odors drive feeding through gustatory receptor neurons in *Drosophila*

Hong-ping Wei[1], Ka Chung Lam[2], and Hokto Kazama[1,3,4,*]

[1]RIKEN Center for Brain Science, Wako, Japan
[2]Division of Life Science, Hong Kong University of Science and Technology, Hong Kong, China
[3]RIKEN CBS-KAO Collaboration Center, Wako, Japan
[4]Graduate School of Arts and Sciences, The University of Tokyo, Tokyo, Japan
[*]Corresponding author: hokto.kazama@riken.jp

Summary

Odors are intimately tied to the taste system to aid food selection and determine the sensory experience of food. However, how smell and taste are integrated in the nervous system to drive feeding behavior remains largely unknown. We show in *Drosophila* that odors alone activate gustatory receptor neurons (GRNs) and trigger proboscis extension reflex (PER), a canonical taste-evoked feeding behavior. Odor-evoked PER requires the function of sugar-sensing GRNs but not the olfactory organs. Calcium imaging shows that GRNs directly respond to odors. Odor-evoked PER is mediated by the Gr5a receptor, and is bidirectionally modulated by specific olfactory binding proteins. Finally, odors and sucrose co-applied to GRNs synergistically enhance PER. These results reveal a cell-intrinsic mechanism for odor-taste multimodal integration that takes place as early as in GRNs, indicating that unified chemosensory experience is a product of layered integration in peripheral neurons and in the brain.

Introduction

Feeding behavior is an outcome of intricate interactions among multiple external and internal senses (Boesveldt and de Graaf, 2017; McCrickerd and Forde, 2016; Spence, 2015). Of particular relevance is an interplay between the senses of smell and taste. Olfactory and gustatory systems prime feeding by signaling food presence, guiding food choice, and inducing anticipatory responses in digestive organs (Boesveldt and de Graaf, 2017; McCrickerd and Forde, 2016). During consumption, they synergistically define the sensory experience of food together with other cues (Spence, 2015). Although imaging studies have identified neural correlates of odor-taste interaction in the brain (Small, 2012), mechanistic understanding of chemosensory integration is lacking in any organism.

Drosophila offers an attractive model to address this issue, where peripheral chemosensory systems are well-characterized (Scott, 2018; Wilson, 2013), and feeding behavior can be quantified using the proboscis extension reflex (PER) (Dethier, 1976). PER is an initial step of feeding evoked by the presentation of sugar to the proboscis or legs housing gustatory receptor neurons (GRNs). Previous studies reported that odors increase the rate of PER (Oh et al., 2021; Reisenman and Scott, 2019; Shiraiwa, 2008), exemplifying olfactory enhancement of feeding in *Drosophila*. However, aside from the involvement of olfactory receptor neurons (Oh et al., 2021; Shiraiwa, 2008), biological mechanisms underlying this multisensory enhancement remain elusive.

Here we investigated the impact of odors on PER and found an unforeseen, direct contribution of GRNs to odor reception, indicating that multisensory integration commences at the very periphery.

Results

Odors alone evoke PER

To examine how odors affect PER, we built a behavioral recording setup in which a tastant and multiple odors with diverse innate values (Badel et al., 2016) can be applied to individual, tethered flies (Figure 1A). To quantify the movement of proboscis, we used a deep learning-based, markerless pose estimation algorithm (Mathis et al., 2018) and tracked the trajectory of three segments constituting the proboscis. The angles made between the segments (rostrum, haustellum, and labellum angles) were subsequently calculated over time to detect PER (Figures 1A-1C; see Methods for the definition of PER). Unexpectedly, we found that the odors alone evoked repetitive PER without an application of a tastant (Figures 1D-1G, and Movie S1). Different odors evoked PER with different probability (Figure 1E), latency (Figure S1A) and duration (Figure 1F and 1G). Stimulus-triggered PER was not observed in response to solvents or air (Figure 1D-1G). Odors evoked PER even at the concentration of 10^{-2}, which was predominantly used to characterize the tuning of olfactory neurons in previous studies (Badel et al., 2016; Endo et al., 2020). The level of PER did not correlate with the innate value of odors (Pearson's $R = 0.33$, $p = 0.52$).

Odor-evoked PER resembled taste-evoked PER in multiple aspects. First, its trajectory was similar to that of taste-evoked PER (Figure S1B) and was consistent with the previously reported movement of proboscis during sucrose-evoked PER (Schwarz et al., 2017). The trajectories were also indistinguishable between all the tested odors (Figure S1B). Second, it showed concentration dependency (Dethier, 1976; Wang et al., 2004). The probability and duration of PER increased as a function of stimulus concentration (Figures 1E and 1G). Third, it depended on the metabolic state just as taste-evoked PER (Inagaki et al., 2014). The duration of PER was higher in starved as compared to fed flies (Figure S2).

In sum, odors initiate feeding behavior in *Drosophila*.

Odors evoke PER through GRNs

To confirm that this behavior is mediated by the olfactory system, we repeated the experiment after removing the sensory organs housing the olfactory receptor neurons, namely the antennae and the maxillary palps. However, this manipulation only attenuated and did not eliminate odor-evoked PER (Figure 2A). Suppressing the activity of most olfactory receptor neurons by expressing a potassium channel Kir2.1 (Paradis et al., 2001) with *Orco-Gal4* driver (Larsson et al., 2004) gave similar results (Figures 2B and 2C). These data show that the olfactory system modulates but is not required for odor-evoked PER.

We thus turned to another chemosensory system, the gustatory system. To examine its involvement in odor-evoked PER, we expressed Kir2.1 in different types of GRNs using type-specific Gal4 drivers, each of which mediates a specific taste modality (Scott, 2018). Gr5a GRNs detect sugar and mediate food acceptance behaviors including PER (Dahanukar et al., 2001; Wang et al., 2004). Suppression of Gr5a GRNs significantly reduced odor-evoked PER, indicating that sweet-sensing neurons detect odors and drive PER (Figures 2B and 2D). Bitter-sensing Gr66a GRNs, on the other hand, have been shown to inhibit sweet-evoked PER (Wang

et al., 2004). However, expression of Kir2.1 in these neurons had little effect (Figures 2B and 2E). We hypothesized that this is due to our use of starved flies because Gr66a pathway is reported to be downregulated in the starved condition (Devineni et al., 2019; Inagaki et al., 2014). Indeed, flies of the same genotype showed increased PER to odors in a fed state (Figure 2H), indicating that Gr66a GRNs counteract PER. Two other tastes, water and low salt can also induce PER (Cameron et al., 2010; Wang et al., 2004), which are detected by Ppk28 and Ir94e GRNs, respectively (Cameron et al., 2010; Jaeger et al., 2018). However, suppression of these cell types did not affect odor-evoked PER (Figures 2B, 2F and 2G). Together, Gr5a GRNs enhance whereas Gr66a GRNs inhibit odor-evoked PER.

As GRNs are housed in multiple external organs including the labella at the tip of proboscis, the legs, the wing margins, and the ovipositor (Scott, 2018), we next sought to narrow down the GRNs responsible for odor-evoked PER. We found that removal of the legs and wings did not abolish the behavior (Figure S3). Moreover, activation of the ovipositor induces egg laying rather than PER (Dethier, 1976). These results suggest that GRNs act predominantly in the labellum to induce odor-evoked PER.

Gustatory receptors and olfactory binding proteins mediate odor-evoked PER

We have shown that Gr5a GRNs tuned to certain sweet tastes trigger PER in response to a wide range of odors. Because GRNs do not express olfactory receptors (Davie et al., 2018; Li et al., 2021; Scott et al., 2001), either gustatory receptors or some other molecules are likely to interact with odorants (Jones et al., 2007; Kwon et al., 2007). Gr5a receptor is a primary candidate as Gr5a GRNs are the positive driver of odor-evoked PER (Figures 2B and 2D). Consistent with this hypothesis, odor-evoked PER was nearly undetectable in the Gr5a mutant but spared in the control (Figure 2I). This demonstrates that Gr5a receptor is necessary for odor-evoked PER.

Odorant binding proteins (OBPs) are another set of molecules that could mediate odor detection by GRNs. They are thought to bind and help transport hydrophobic odorants to chemosensory receptors through aqueous lymph (Larter et al., 2016). OBPs are expressed in taste as well as olfactory sensilla (Galindo and Smith, 2001) and modulate sugar-evoked PER (Swarup et al., 2014), raising the possibility that those in the taste sensilla also mediate odorant detection. To test this, we conducted a genetic screen by expressing individual Obp RNAi constructs with *tubulin-Gal4*. We targeted 9 Obp genes that are expressed highly in the labellum (Cameron et al., 2010) but in trace amounts in the antenna(Larter et al., 2016) to examine the function of OBPs in the taste sensilla. Knockdown of *Obp18a*, *Obp57d/e*, and *Obp57e* genes decreased whereas that of *Obp49a* gene increased odor-evoked PER (Figures 2J and 2K, and Figure S4). Knockdown of *Obp19b*, *Obp56g*, *Obp56h*, *Obp57a/c*, and *Obp83c* genes did not have a significant effect on odor-evoked PER (Figure 2L, and Figure S4). The increased PER following *Obp49a* knockdown likely reflects disinhibition of sweet-sensing GRNs as Obp49a mediates the inhibitory impact of bitter chemicals on the activity of sweet-sensing GRNs (Jeong et al., 2013). These results suggest that OBPs modulate odor detection by GRNs.

GRNs respond to odors

To gain direct evidence that GRNs respond to odors, we performed two-photon calcium imaging of GRN axons in the subesophageal zone of the brain (Figure 3A). A genetically-encoded calcium indicator GCaMP6s (Chen et al., 2013) was expressed in Gr5a, Gr66a, Ppk28, or Ir94e GRNs. Consistent with the contribution of Gr5a and Gr66a GRNs to odor-evoked PER, robust odor responses were observed in these neurons. They responded to all the tested odors but not to

control stimuli, with distinct tuning (Figures 3B-3F and Figures S5A-S5F), in a concentration-dependent manner (Figures S5G and S5H). A linear combination of these GRN responses well predicted the magnitude of odor-evoked PER (Figure 3G). By contrast, Ppk28 and Ir94e GRNs did not respond to any odors (Figures S5I and S5J), matching their little contribution to odor-evoked PER (Figures 2B, 2F and 2G).

These responses could reflect the activity originating in GRNs or that from a central olfactory circuit impinging on GRN's presynaptic terminals. To distinguish between the two scenarios, we physically covered the maxillary palps to block the input from the olfactory organs and applied odors (antennae were already removed to gain optical access to the subesophageal zone, see Methods). This manipulation had little effect on the odor responses (Figure 3D and 3F). On the other hand, the responses were eliminated after covering the labella (Figures 3D and 3F), demonstrating that GRNs themselves sense odors.

As we observed that Gr5a receptor was necessary for odor-evoked PER, we further asked whether it is required for Gr5a GRNs to respond to odors. We found that odor responses were absent in the Gr5a mutant but spared in control flies (Figure 3H). This confirms that odor responses in Gr5a GRNs depend on Gr5a receptor.

GRNs integrate odor-taste multisensory input

Having observed that GRNs detect odors besides tastants, we finally examined if GRNs can integrate these stimuli of different sensory modalities and enhance PER. We decided to apply a mix of banana odor and sucrose as a mimic of multisensory food stimuli in the natural environment. We confirmed that the banana odor can evoke PER and GRN responses in a concentration-dependent manner (Figures S6A and S6B). We then presented sucrose solution mixed with or without a low concentration (10^{-4}) of banana odor locally to the labellum (Figure 4A). Although banana odor could not evoke PER on its own at this concentration (Figure S6A), we found that the addition of banana odor increased PER to sucrose especially at low concentrations where sucrose alone can only induce unreliable PER (Figure 4B). Importantly, this enhancement was observed even after removing the olfactory organs (Figure 4B), indicating that the superadditive integration takes place in GRNs. Similar results were obtained when sucrose was mixed with different monomolecular odorants (Figures S6C and S6D). Thus, GRNs serve as an initial node for odor-taste multisensory integration that shapes feeding behavior.

Discussion

In terrestrial animals, it has been considered that there is a clear division of labor between the two types of chemosensory organs in sensing stimuli with distinct physical properties; the olfactory and gustatory organs sense volatile and non-volatile chemicals, respectively. Therefore, although odorants and tastants are defined by the identity of cognate organs, they are used interchangeably with volatile and non-volatile chemicals. However, we found that GRNs directly detect odorants, and this drives a classical taste-induced feeding behavior, PER. Thus, volatile chemicals are within the molecular receptive range of GRNs and should also be regarded as tastants based on the conventional definition. Critically, this indicates that GRNs are engaged in non-contact chemo-sensing as well, a behavioral strategy distinct from contact-based chemo-sensing.

Our results showed that odor responses of Gr5a GRNs are mediated by Gr5a receptor. This may not be totally enigmatic as gustatory and olfactory receptor genes belong to the same ancient superfamily sharing a motif in the transmembrane region (Robertson et al., 2003; Scott et

al., 2001), and some gustatory receptors expressed outside of GRNs function in odor (Jones et al., 2007; Kwon et al., 2007), temperature (Ni et al., 2013), and light detection (Montell, 2021; Xiang et al., 2010). However, Gr5a is unique in that the same receptor can detect stimuli of two different sensory modalities. Furthermore, we found that OBPs enriched in the labellum modulate odor-evoked PER, suggesting that OBPs in this taste organ not only link tastants with gustatory receptors (Jeong et al., 2013; Swarup et al., 2014), but also mediate detection of odors. These data illuminate a novel role of GRNs in feeding behavior of *Drosophila* in natural settings. During foraging in the air, olfactory receptor neurons that are more sensitive to odors locate a potential food source together with other sensory systems. After landing on the potential food, GRNs on the legs join to assess its edibility. In parallel, GRNs on the labella sense odors and enhance the probability of PER. Given that the olfactory system most likely has already guided the animal to palatable food, keeping the GRNs broadly tuned to odors is an efficient mechanism to enhance PER. Once PER brings the labella into contact with the food, GRNs act as a multisensory integrator to make a decision on food intake (Figure 4C). Because inputs from olfactory and gustatory organs interact centrally as well (Oh et al., 2021; Shiraiwa, 2008) (Figure 2A), this indicates that unified chemosensory experience is built through layered integration in different parts of the body.

Although odor detection by GRNs through gustatory receptors has not previously been reported, olfactory receptors have been shown to be expressed in the proboscis in multiple insects (Haverkamp et al., 2016; Kwon et al., 2006; Xia and Zwiebel, 2006). A recent study reported that olfactory receptors are also expressed and functional in cultured human fungiform and mouse taste papilla cells (Malik et al., 2019), implying that peripheral odor-taste integration may be a process incorporated in various species. These and our results reveal that GRNs should be further studied not as gustatory neurons but more broadly as chemosensory integrators.

Acknowledgments

We thank Anupama Dahanukar, Graeme Davis, Michael Dickinson, Craig Montell, Kristin Scott, the Bloomington Stock Center, and the Vienna Drosophila Resource Center for flies; RIKEN CBS-Olympus Collaboration Center for imaging equipment and software; members of the Kazama laboratory for their support and comments on the manuscript. HP.W. was supported by Grant-in-Aid for JSPS Research Fellow (JP15F15384) and RIKEN Special Postdoctoral Fellowship. This work was supported by a grant from RIKEN, Kao Corporation, and JSPS KAKENHI Grant (JP18H02532, JP18K19502, JP21H04789) to H.K.

Author contributions

HP.W. and H.K. designed the study. HP.W. performed all the experiments and analyzed data except for part of the behavioral data analysis, which was performed by K.C.L. HP.W. and H.K. wrote the paper with input from K.C.L.

Declaration of interests

Authors declare that they have no competing interests.

Data and code availability

Data are available from the corresponding author on request. Analysis code is available at: https://github.com/hpwei82/2022_hpwei

Supplemental information

Supplemental information includes six figures and one movie.

Materials and Methods

Fly stocks and husbandry

Flies were maintained on standard cornmeal agar under a 12 h light, 12 h dark cycle at 25 °C. All experiments were performed on adult females 2–6 days after eclosion.

Fly stocks used in this study are as follows: Dickinson wild type (Michael Dickinson), *tubulin-GAL4* (Bloomington #5138 (Lee and Luo, 1999)), *Orco-GAL4* (Bloomington #26818 (Larsson et al., 2004)), *Gr66a-GAL4* (Bloomington #57670 (Kwon et al., 2011)), *Ir94e-GAL4* (Bloomington #60725 (Jaeger et al., 2018)), *Ppk28-GAL4* (Bloomington #93020 (Cameron *et al*., 2010)), *UAS-GCaMP6s* (Bloomington #42746, 42749 (Chen et al., 2013)), *UAS-Obp49a RNAi* (VDRC #330599 (Dietzl et al., 2007)), *UAS-Obp19b RNAi* (VDRC #1823), *UAS-Obp56g RNAi* (VDRC #23206), *UAS-Obp56h RNAi* (VDRC #102562), *UAS-Obp18a RNAi* (VDRC #101628), *UAS-Obp83c RNAi* (VDRC #106866), *UAS-Obp57d/e RNAi* (VDRC #101783), *UAS-Obp57e RNAi* (VDRC #105001), *UAS-Obp57a/c RNAi* (VDRC #107489), three OBP RNAi control lines w^{1118} (VDRC #60000, control for *UAS-Obp19b RNAi* and *UAS-Obp56g RNAi*), w^{1118}*;P{VDRCsh60200attP40* (VDRC #60200, control for *UAS-Obp49a RNAi*), *y,*w^{1118}*;P{attP,y[+],w[3']}* (VDRC #60100, control for other *UAS-Obp RNAi* lines), *Gr5a-GAL4* (Kristin Scott), Gr5a mutant (Anupama Dahanukar (Dahanukar et al., 2007), *ΔEP(x)-5*) and its control (Anupama Dahanukar (Dahanukar et al., 2007), *EP(x)496*), and *UAS-Kir2.1*^{AAE}*-GFP* (Graeme Davis (Paradis et al., 2001)). All the lines except for *Gr5a* mutant, its control, and the UAS-RNAi lines were backcrossed for 6 generations to the Dickinson wild type (Dickinson, 1999).

Detailed genotypes of flies used in each experiment are listed in Table 1.

Figure	**Short genotype**
1B-1G, 2A, 4B, S1A-S1B, S2A-S2B, S6A, S6C, S6D	Dickinson Wild type
2B, 2C	*UAS-Kir2.1/+*
2C, S3A, S3B	*Orco-Gal4/UAS-Kir2.1*
2D	*Gr5a-Gal4/UAS-Kir2.1*
2E, 2H	*Gr66a-Gal4/UAS-Kir2.1*
2F	*Ppk28-Gal4/UAS-Kir2.1*
2G	*Ir94e-Gal4/UAS-Kir2.1*
2I	*ΔEP(x)-5* *EP(x)496*
2J, S4C	*tubulin-Gal4/y,*w^{1118}*;P{attP,y[+],w[3']}*
2J	*tubulin-Gal4/UAS-Obp57d/e RNAi*

2K	*tubulin-Gal4/w^{1118};P{VDRCsh60200}xattP40*
	tubulin-Gal4/UAS-Obp49a RNAi
2L, S4A	*tubulin-Gal4/w^{1118}*
2L	*tubulin-Gal4/UAS-Obp19b RNAi*
3A-3D, 3G, S5A-S5C, S5G, S6B	*Gr5a-Gal4;UAS-GCaMP6s*
3E, 3F, S5D-S5F, S5H	*UAS-GCaMP6s;Gr66a-Gal4*
3H	*ΔEP(x)-5;Gr5a-Gal4;UAS-GCaMP6s* *EP(x)496;Gr5a-Gal4;UAS-GCaMP6s*
S4B	*tubulin-Gal4/UAS-Obp56g RNAi*
S4D	*tubulin-Gal4/UAS-Obp18a RNAi*
S4E	*tubulin-Gal4/UAS-Obp56h RNAi*
S4F	*tubulin-Gal4/UAS-Obp83c RNAi*
S4G	*tubulin-Gal4/UAS-Obp57e RNAi*
S4H	*tubulin-Gal4/UAS-Obp57a/c RNAi*
S5J	*UAS-GCaMP6s;Ppk28-Gal4*
S5J	*UAS-GCaMP6s;Ir94e-Gal4*

Table 1. Genotypes used to generate data presented in each figure.

Examination of odor-evoked PER

Virgin females that had been raised on food for 1-3 days were starved for 24-28 h in vials with water supplied through a wet piece of Kimwipe. Individual flies were briefly anesthetized on ice and their dorsal side of the thorax was attached to a cover glass with ultraviolet-curing adhesive (NOA 63, Norland), after which the flies were allowed to rest for an hour. Prior to recording odor-evoked PER, flies were water satiated until they did not consume any more. Subsequently, 100 mM sucrose solution, which acted as a positive control stimulus, was applied either on the fly's legs or proboscis (without letting the fly consume it) to examine if the fly could exhibit tastant-evoked PER. Flies were discarded if they did not exhibit PER to this stimulus. Flies showing excessive spontaneous PER before the assay were also discarded. The tethered fly was positioned horizontally in air facing an odor delivery tube (Figure 1A). The tip of the odor tube was placed 10 mm away from the fly. A monochrome camera (Lu070M, Lumenera corporation) taking a lateral view of the fly at 20 Hz was used to record the movement of proboscis in response to odors.

To examine the contribution of olfactory organs to odor-evoked PER (Figures 2, 4 and Figure S6), the third antennal segments and maxillary palps were removed with forceps while the flies were anesthetized on ice. After the surgery, the flies were given an hour to recover before the experiment.

To examine the contribution of GRNs on wings and legs to odor-evoked PER (Figure S3), wings and tarsal segments were removed with forceps while the flies were anesthetized on ice. After the surgery, the flies were given an hour to recover before the experiment.
Individual flies went through an experiment consisting of three blocks. In each block, 6 odors (see below), two solvent controls (mineral oil and water), and another control stimulus (air) were applied for 2 s per trial in a randomized order with a 15 s inter-trial-interval.

Olfactory stimulation

Odors were delivered with a custom-made, multi-channel olfactometer controlled by a PC as previously described. Briefly, an air stream (300 ml/min) was passed through 4 ml of odor solution diluted with mineral oil (nacalai tesque, 23334-85) or water. The concentration of odor was varied between 10^{-4}, 10^{-2}, 10^{-1}, and 0.5 (v/v), but the default was 0.5 unless otherwise noted. The odorized air was further diluted by mixing it with a main air stream (500 ml/min), a small portion of which was delivered frontally to the fly through an outlet placed 10 mm away from the fly. The speed of odorized air flow at the position of the fly was 0.6 m/s. Using the photoionization detector (200B miniPID, Aurora Scientific Inc.), the time odors reach the position of the fly was estimated to be 1.1 s after the odor valve opening. The odors used in the study and their abbreviations are as follows: 2-pentanone (2PT, Wako, 13303743), 3-octanol (OCT, Tokyo chemical industry, O0121), 4-methylcyclohexanol (MCH, Sigma-Aldrich, 153095), banana essence (Narizuka corporation), benzaldehyde (BNZ, Sigma-Aldrich, 418099), ethyl butyrate (EBR, Sigma-Aldrich, E15701), and isopentyl acetate (IPA, Wako, 016-03646).

Examination of multisensory PER

To examine how flies respond to odor-taste multimodal stimuli presented to GRNs in the labellum, individual flies were gently attached to a cover glass vertically by wrapping their thorax with a piece of parafilm, and multimodal stimuli were applied by touching the ventral part of the labellum with a wick made of Kimwipe immersed in a sucrose solution with or without odors (Figure 4A; (Shiraiwa, 2008)). A constant air stream was applied from behind the wick. The legs of the flies were tucked under the parafilm to prevent them from touching the wick. The flies were allowed to rest for an hour after fixation. The concentration of sucrose was varied between 0.25-2% (v/v, Figure 4B) or fixed at 0.25% (Figures S6C and S6D) depending on the experiment. When the concentration of sucrose was varied, the stimuli were applied in an ascending order to avoid adaptation. The concentration of the added odor was 10^{-4} for all the tested stimuli. Each stimulus was applied 3 times with an inter-trial-interval of 15 s. PER was manually scored when the proboscis was fully extended within ~2 s from the stimulation.

Quantification of PER

A markerless pose estimation algorithm DeepLabCut v2.0 was used to quantify the movement of the proboscis. The position and orientation of three segments of the proboscis, the rostrum, the haustellum, and the labellum were characterized by tracking six points, namely the proximal end of the antenna, the distal end of the antenna, the rostrum apex, the rostrum-haustellum joint, the haustellum-labellum joint, and the distal end of the labellum (Figures 1B and 1C). These six points were manually labeled on the lateral view of the fly to generate the training dataset, which consisted of 1465 labeled frames in video data from 19 flies. The ResNet50 based pose estimation neural network was trained for about 200,000 iterations, after which the six points were automatically tracked in all the frames in video data.

Following the pose estimation, data were analyzed using custom code written in Python. To detect proboscis extensions, the rostrum angle (the angle made by the line passing through the proximal and distal ends of the antenna and the line along the rostrum), the haustellum angle (the angle between the rostrum and the haustellum), and the labellum angle (the angle between the haustellum and the labellum) were calculated over time (see Figure 1B). The baseline of each proboscis angle was calculated as the 25th percentile of a rolling 5 s time window. The proboscis extension was defined as PER if the haustellum angle exceeded 100° because it corresponded to full extension by visual inspection. PER duration was defined as the time during which the fly

exhibited PER in each second. Integrated PER duration was defined as the sum of PER duration over 4 s starting 1 s after the odor onset. These values were averaged across three trials for each odor in each fly. PER probability was defined as the percentage of trials in which PER was observed for each stimulus in each fly.

Because repetitive, spontaneous PER occurring at regular intervals represented an abnormal condition, flies showing such repetitive, spontaneous PER in more than 9 trials were excluded from further analysis.

To examine if the movement of the proboscis is similar between odor-evoked and tastant-evoked PER as well as between PER evoked by different odors, temporal sequences of the rostrum and the haustellum angles during PER and partial proboscis extensions were clustered with K-medoids clustering (Park and Jun, 2009). PER and partial proboscis extensions were detected from the baseline subtracted rostrum angle using hysteresis thresholding with a lower threshold of 5° and an upper threshold of 15°. Because the length of a temporal sequence is different between PER, the data were converted to a distance metric using dynamic time warping (Mearns et al., 2020; Sakoe and Chiba, 1978) with a warping window of 0.25 s prior to clustering. The optimal number of clusters was determined using the elbow method.

Immunohistochemistry

To examine the expression pattern of Gal4 driver lines, we performed immunohistochemistry as described previously (Badel et al., 2016) using rat anti-GFP (1:1,000, nacalai tesque, 04404-84) and mouse nc82 (1:20, Developmental Studies Hybridoma Bank at Univ. of Iowa) as primary antibodies, and anti-rat CF488A (1:250, Biotium, 20023) and anti-mouse CF633 (1:250, Biotium, 20120) as secondary antibodies. Brains were dissected out from the head capsule in phosphate-buffered saline (PBS, nacalai tesque, 2757531), fixed with 4% paraformaldehyde in PBS (nacalai tesque, 915414) for 90 min on ice, and incubated in blocking solution containing 5% normal goat serum (Invitrogen, 50197Z) in PBST (0.2% Triton X-100 (nacalai tesque, 3550102) in PBS) for 30 min. Primary antibodies were then added and incubated at 4 ^{o}C for ~48 h. After removing antibodies and washing over an hour, the brains were incubated in a solution of secondary antibodies at 4 ^{o}C for 24 h. The brains were immersed in Vectashield (Vector laboratories, H-1000), sealed with a cover glass, and imaged with a confocal microscope (FV3000, Olympus). Images were analyzed with Fiji (Schindelin et al., 2012).

Fly preparation for calcium imaging

Individual flies starved for 24-28 h with water were anesthetized on ice, and their dorsal side of the thorax was fixed to a piece of parafilm with ultraviolet-curing adhesive (NOA 63, Norland). The legs of the fly were covered with another piece of parafilm. The fly was subsequently attached to a custom-made recording plate in a vertical position such that the anterior part of the head was accessible through a small hole on the recording plate (Figure 3A). The proboscis was pulled out gently with forceps and immobilized in an extended position using a strip of parafilm with the labellum exposed to the air. After covering the head with saline containing 103 mM NaCl, 3 mM KCl, 5 mM N-tris (hydroxymethyl) methyl-2-aminoethane-sulfonic acid, 8 mM trehalose, 10 mM glucose, 26 mM $NaHCO_3$, 1 mM NaH_2PO_4, 1.5 mM $CaCl_2$, and 4 mM $MgCl_2$ (osmolarity adjusted to 270-275 mOsm), the antennae and the associated cuticle were removed to expose the subesophageal zone. Saline was bubbled with 95% O_2/5% CO_2 and perfused at a rate of 2 ml/min during the recording.

Two-photon calcium imaging

Calcium imaging of GRN axons in the subesophageal zone was conducted using a two-photon microscope (LSM 7 MP, Zeiss) equipped with a piezo motor (P-725.2CD PIFOC, PI) that drives a water immersion objective lens (W Plan-Apochromat, 20x, numerical aperture 1.0) along the z-axis. The fluorophore was excited with a titanium:sapphire pulsed laser (Chameleon Vision II, Coherent) mode-locked at 930 nm. The laser power measured at the back aperture of the objective lens was below 20 mW. Fluorescence was collected with a GaAsP detector through a bandpass emission filter (BP470-550). Five optical slices separated by 5 μm were scanned every 500 ms. The odor delivery system was identical to that used in behavioral experiments.

Image processing

Calcium imaging data were analyzed using custom code written in MATLAB (MathWorks). Images were registered within and across trials to correct for movement in the x-y plane as well as in depth by determining the shift along three dimensions that maximizes the correlation between the images. The region of interest (ROI) was set to cover the GRN axons in the subesophageal zone. The size of ROI was 80 x 60 μm for Gr5a GRNs, 60 x 40 μm for Gr66a GRNs, 80 x 60 μm for Ir94e GRNs, and 80 x 40 μm for Ppk28 GRNs, respectively. The average pixel intensity within the ROI was calculated for each time frame. The average of 5 frames preceding a stimulus was used as the baseline signal to calculate $\Delta F/F$ for each time frame. The peak stimulus response was quantified by averaging $\Delta F/F$ across five frames at the peak, followed by averaging across three trials for each stimulus.

Statistical analysis

Statistical analyses described in figure legends were preformed using Python or R. A linear model in Figure 3G was generated using Python scikit-learn. Sample sizes are listed in figure legends.

References

Badel, L., Ohta, K., Tsuchimoto, Y., and Kazama, H. (2016). Decoding of Context-Dependent Olfactory Behavior in Drosophila. Neuron *91*, 155-167. 10.1016/j.neuron.2016.05.022.

Boesveldt, S., and de Graaf, K. (2017). The Differential Role of Smell and Taste For Eating Behavior. Perception *46*, 307-319. 10.1177/0301006616685576.

Cameron, P., Hiroi, M., Ngai, J., and Scott, K. (2010). The molecular basis for water taste in Drosophila. Nature *465*, 91-95. 10.1038/nature09011.

Chen, T.W., Wardill, T.J., Sun, Y., Pulver, S.R., Renninger, S.L., Baohan, A., Schreiter, E.R., Kerr, R.A., Orger, M.B., Jayaraman, V., et al. (2013). Ultrasensitive fluorescent proteins for imaging neuronal activity. Nature *499*, 295-300. 10.1038/nature12354.

Dahanukar, A., Foster, K., van der Goes van Naters, W.M., and Carlson, J.R. (2001). A Gr receptor

is required for response to the sugar trehalose in taste neurons of Drosophila. Nat Neurosci *4*, 1182-1186. 10.1038/nn765.

Dahanukar, A., Lei, Y.T., Kwon, J.Y., and Carlson, J.R. (2007). Two Gr genes underlie sugar reception in Drosophila. Neuron *56*, 503-516. 10.1016/j.neuron.2007.10.024.

Davie, K., Janssens, J., Koldere, D., De Waegeneer, M., Pech, U., Kreft, L., Aibar, S., Makhzami, S., Christiaens, V., Bravo Gonzalez-Blas, C., et al. (2018). A Single-Cell Transcriptome Atlas of the Aging Drosophila Brain. Cell *174*, 982-998 e920. 10.1016/j.cell.2018.05.057.

Dethier, V.G. (1976). The hungry fly: A physiological study of the behavior associated with feeding.

Devineni, A.V., Sun, B., Zhukovskaya, A., and Axel, R. (2019). Acetic acid activates distinct taste pathways in Drosophila to elicit opposing, state-dependent feeding responses. Elife *8*. 10.7554/eLife.47677.

Dickinson, M.H. (1999). Haltere-mediated equilibrium reflexes of the fruit fly, Drosophila melanogaster. Philos Trans R Soc Lond B Biol Sci *354*, 903-916. 10.1098/rstb.1999.0442.

Dietzl, G., Chen, D., Schnorrer, F., Su, K.C., Barinova, Y., Fellner, M., Gasser, B., Kinsey, K., Oppel, S., Scheiblauer, S., et al. (2007). A genome-wide transgenic RNAi library for conditional gene inactivation in Drosophila. Nature *448*, 151-156. 10.1038/nature05954.

Endo, K., Tsuchimoto, Y., and Kazama, H. (2020). Synthesis of Conserved Odor Object Representations in a Random, Divergent-Convergent Network. Neuron *108*, 367-381 e365. 10.1016/j.neuron.2020.07.029.

Galindo, K., and Smith, D.P. (2001). A large family of divergent Drosophila odorant-binding proteins expressed in gustatory and olfactory sensilla. Genetics *159*, 1059-1072. 10.1093/genetics/159.3.1059.

Haverkamp, A., Yon, F., Keesey, I.W., Mißbach, C., Koenig, C., Hansson, B.S., Baldwin, I.T., Knaden, M., and Kessler, D. (2016). Hawkmoths evaluate scenting flowers with the tip of their proboscis. Elife *5*, e15039.

Inagaki, H.K., Panse, K.M., and Anderson, D.J. (2014). Independent, reciprocal neuromodulatory control of sweet and bitter taste sensitivity during starvation in Drosophila. Neuron *84*, 806-820. 10.1016/j.neuron.2014.09.032.

Jaeger, A.H., Stanley, M., Weiss, Z.F., Musso, P.Y., Chan, R.C., Zhang, H., Feldman-Kiss, D., and Gordon, M.D. (2018). A complex peripheral code for salt taste in Drosophila. Elife *7*. 10.7554/eLife.37167.

Jeong, Y.T., Shim, J., Oh, S.R., Yoon, H.I., Kim, C.H., Moon, S.J., and Montell, C. (2013). An odorant-binding protein required for suppression of sweet taste by bitter chemicals. Neuron *79*, 725-737. 10.1016/j.neuron.2013.06.025.

Jones, W.D., Cayirlioglu, P., Kadow, I.G., and Vosshall, L.B. (2007). Two chemosensory receptors

together mediate carbon dioxide detection in Drosophila. Nature *445*, 86-90. 10.1038/nature05466.

Kwon, H.W., Lu, T., Rutzler, M., and Zwiebel, L.J. (2006). Olfactory responses in a gustatory organ of the malaria vector mosquito Anopheles gambiae. Proc Natl Acad Sci U S A *103*, 13526-13531. 10.1073/pnas.0601107103.

Kwon, J.Y., Dahanukar, A., Weiss, L.A., and Carlson, J.R. (2007). The molecular basis of CO2 reception in Drosophila. Proc Natl Acad Sci U S A *104*, 3574-3578. 10.1073/pnas.0700079104.

Kwon, J.Y., Dahanukar, A., Weiss, L.A., and Carlson, J.R. (2011). Molecular and cellular organization of the taste system in the Drosophila larva. J Neurosci *31*, 15300-15309. 10.1523/JNEUROSCI.3363-11.2011.

Larsson, M.C., Domingos, A.I., Jones, W.D., Chiappe, M.E., Amrein, H., and Vosshall, L.B. (2004). Or83b encodes a broadly expressed odorant receptor essential for Drosophila olfaction. Neuron *43*, 703-714. 10.1016/j.neuron.2004.08.019.

Larter, N.K., Sun, J.S., and Carlson, J.R. (2016). Organization and function of Drosophila odorant binding proteins. Elife *5*. 10.7554/eLife.20242.

Lee, T., and Luo, L. (1999). Mosaic analysis with a repressible cell marker for studies of gene function in neuronal morphogenesis. Neuron *22*, 451-461. 10.1016/s0896-6273(00)80701-1.

Li, H., Janssens, J., De Waegeneer, M., Kolluru, S.S., Davie, K., Gardeux, V., Saelens, W., David, F., Brbić, M., and Leskovec, J. (2021). Fly Cell Atlas: a single-cell transcriptomic atlas of the adult fruit fly. bioRxiv.

Malik, B., Elkaddi, N., Turkistani, J., Spielman, A.I., and Ozdener, M.H. (2019). Mammalian Taste Cells Express Functional Olfactory Receptors. Chem Senses *44*, 289-301. 10.1093/chemse/bjz019.

Mathis, A., Mamidanna, P., Cury, K.M., Abe, T., Murthy, V.N., Mathis, M.W., and Bethge, M. (2018). DeepLabCut: markerless pose estimation of user-defined body parts with deep learning. Nat Neurosci *21*, 1281-1289. 10.1038/s41593-018-0209-y.

McCrickerd, K., and Forde, C.G. (2016). Sensory influences on food intake control: moving beyond palatability. Obes Rev *17*, 18-29. 10.1111/obr.12340.

Mearns, D.S., Donovan, J.C., Fernandes, A.M., Semmelhack, J.L., and Baier, H. (2020). Deconstructing Hunting Behavior Reveals a Tightly Coupled Stimulus-Response Loop. Curr Biol *30*, 54-69 e59. 10.1016/j.cub.2019.11.022.

Montell, C. (2021). Drosophila sensory receptors-a set of molecular Swiss Army Knives. Genetics *217*, 1-34. 10.1093/genetics/iyaa011.

Ni, L., Bronk, P., Chang, E.C., Lowell, A.M., Flam, J.O., Panzano, V.C., Theobald, D.L., Griffith, L.C., and Garrity, P.A. (2013). A gustatory receptor paralogue controls rapid warmth avoidance in Drosophila. Nature *500*, 580-584. 10.1038/nature12390.

Oh, S.M., Jeong, K., Seo, J.T., and Moon, S.J. (2021). Multisensory interactions regulate feeding behavior in Drosophila. Proc Natl Acad Sci U S A *118*. 10.1073/pnas.2004523118.

Paradis, S., Sweeney, S.T., and Davis, G.W. (2001). Homeostatic control of presynaptic release is triggered by postsynaptic membrane depolarization. Neuron *30*, 737-749. 10.1016/s0896-6273(01)00326-9.

Park, H.-S., and Jun, C.-H. (2009). A simple and fast algorithm for K-medoids clustering. Expert systems with applications *36*, 3336-3341.

Reisenman, C.E., and Scott, K. (2019). Food-derived volatiles enhance consumption in Drosophila melanogaster. J Exp Biol *222*. 10.1242/jeb.202762.

Robertson, H.M., Warr, C.G., and Carlson, J.R. (2003). Molecular evolution of the insect chemoreceptor gene superfamily in Drosophila melanogaster. Proc Natl Acad Sci U S A *100 Suppl 2*, 14537-14542. 10.1073/pnas.2335847100.

Sakoe, H., and Chiba, S. (1978). Dynamic programming algorithm optimization for spoken word recognition. IEEE transactions on acoustics, speech, and signal processing *26*, 43-49.

Schindelin, J., Arganda-Carreras, I., Frise, E., Kaynig, V., Longair, M., Pietzsch, T., Preibisch, S., Rueden, C., Saalfeld, S., Schmid, B., et al. (2012). Fiji: an open-source platform for biological-image analysis. Nat Methods *9*, 676-682. 10.1038/nmeth.2019.

Schwarz, O., Bohra, A.A., Liu, X., Reichert, H., VijayRaghavan, K., and Pielage, J. (2017). Motor control of Drosophila feeding behavior. Elife *6*. 10.7554/eLife.19892.

Scott, K. (2018). Gustatory Processing in Drosophila melanogaster. Annu Rev Entomol *63*, 15-30. 10.1146/annurev-ento-020117-043331.

Scott, K., Brady, R., Jr., Cravchik, A., Morozov, P., Rzhetsky, A., Zuker, C., and Axel, R. (2001). A chemosensory gene family encoding candidate gustatory and olfactory receptors in Drosophila. Cell *104*, 661-673. 10.1016/s0092-8674(01)00263-x.

Shiraiwa, T. (2008). Multimodal chemosensory integration through the maxillary palp in Drosophila. PLoS One *3*, e2191. 10.1371/journal.pone.0002191.

Small, D.M. (2012). Flavor is in the brain. Physiol Behav *107*, 540-552. 10.1016/j.physbeh.2012.04.011.

Spence, C. (2015). Multisensory flavor perception. Cell *161*, 24-35. 10.1016/j.cell.2015.03.007.

Swarup, S., Morozova, T.V., Sridhar, S., Nokes, M., and Anholt, R.R. (2014). Modulation of feeding behavior by odorant-binding proteins in Drosophila melanogaster. Chem Senses

39, 125-132. 10.1093/chemse/bjt061.

Wang, Z., Singhvi, A., Kong, P., and Scott, K. (2004). Taste representations in the Drosophila brain. Cell *117*, 981-991. 10.1016/j.cell.2004.06.011.

Wilson, R.I. (2013). Early olfactory processing in Drosophila: mechanisms and principles. Annu Rev Neurosci *36*, 217-241. 10.1146/annurev-neuro-062111-150533.

Xia, Y., and Zwiebel, L.J. (2006). Identification and characterization of an odorant receptor from the West Nile virus mosquito, Culex quinquefasciatus. Insect Biochem Mol Biol *36*, 169-176. 10.1016/j.ibmb.2005.12.003.

Xiang, Y., Yuan, Q., Vogt, N., Looger, L.L., Jan, L.Y., and Jan, Y.N. (2010). Light-avoidance-mediating photoreceptors tile the Drosophila larval body wall. Nature *468*, 921-926. 10.1038/nature09576.

Figures

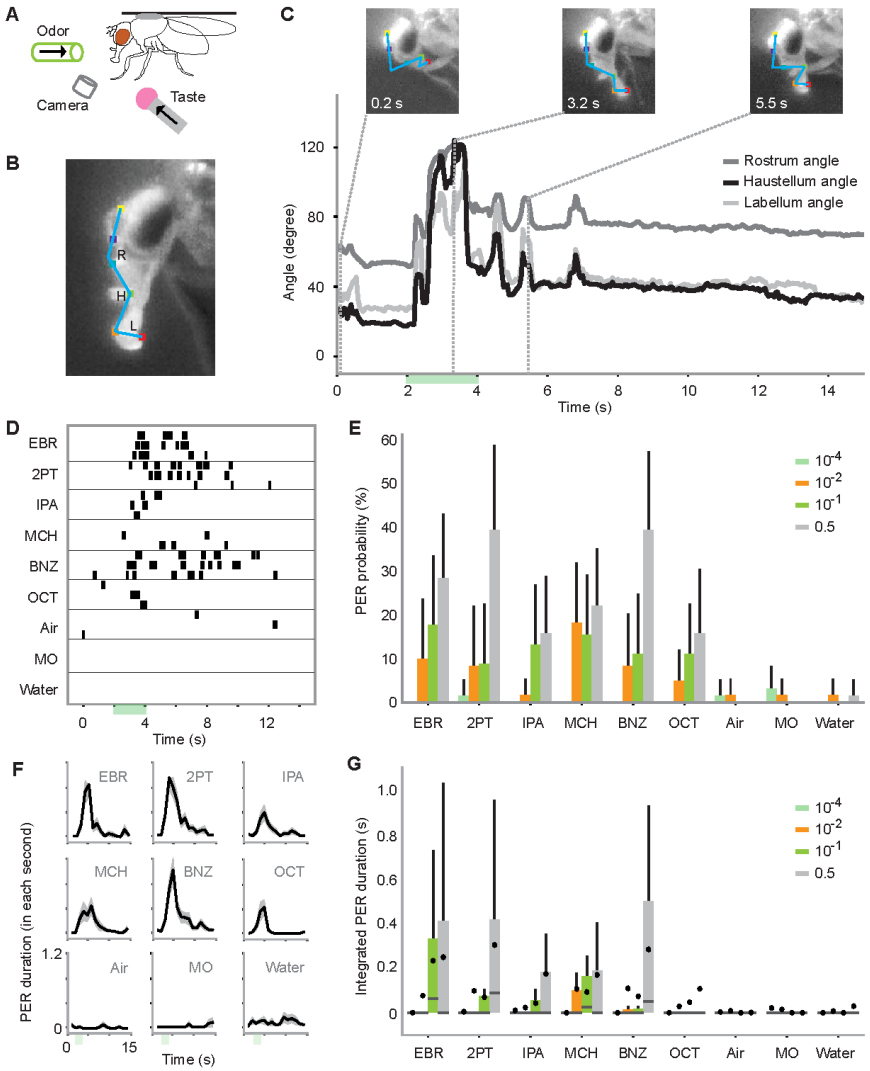

Figure 1. Odors alone initiate PER

(**A**) Schematic for recording odor-evoked PER. (**B**) Six points on the head tracked by DeepLabCut. The movement of the proboscis was characterized by the positions of three segments of the proboscis and the angles between the segments, namely the rostrum angle (R), haustellum angle (H), and labellum angle (L). (**C**) Example odor-evoked PER. Top, images of a proboscis in a retracted (0.2 s), fully extended (3.1 s) and partially extended (5.5 s) state. Bottom, the three angles over time. Green bar indicates an odor application period. Odor is ethyl butyrate. (**D**) PER to nine odors in an example fly. Each row corresponds to a trial and each tick mark indicates the timing of PER. See Materials and Methods for the abbreviations of odors. (**E**) PER probability in wild type flies in response to different concentrations of odors. The same stimulus was used for air, mineral oil, and water controls. n = 21, 26, 27, and 28 flies for 10^{-4}, 10^{-2}, 10^{-1}, and 0.5 concentration groups, respectively. Error bar, standard error of the mean. **(F)** PER duration in wild type flies. The black lines indicate the mean and the shaded areas indicate the 95% confidence interval. n = 28 flies. (**G**) Integrated PER duration in wild type flies in response

to different concentrations of odors. The data is from the same flies as in **E**. Box plots indicate the median (gray line), mean (black dot), quartiles (box), and 5-95% range (bar).

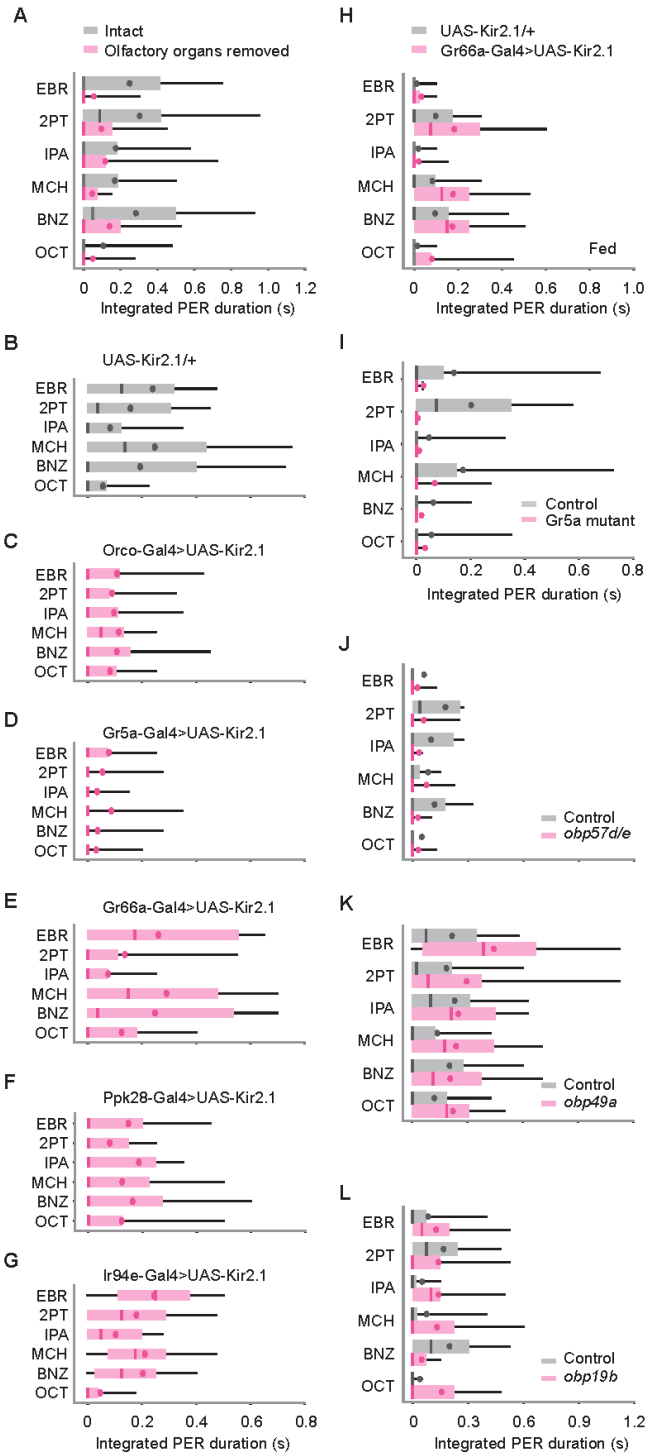

Figure 2. Odors evoke PER through GRNs

(**A**) Integrated PER duration in intact (n = 28) and olfactory organs removed (n = 32) wild type flies. Flies with olfactory organs removed show less PER compared to control flies. p = 0.005.

(**B-G**) Integrated PER duration in control (*UAS-Kir2.1*/+, n = 20, **B**), Orco ORN silenced (Orco-Gal4>UAS-Kir2.1, n = 24, **C**), and GRN silenced (Gr5a-Gal4>UAS-Kir2.1, n = 25, **D**; Gr66a-Gal4>UAS-Kir2.1, n = 24, **E**; Ppk28-Gal4>UAS-Kir2.1, n = 28, **F**; Ir94e-Gal4>UAS-Kir2.1, n = 23, **G**) flies. Each silenced line was compared to the control in **B**. p = 0.06, 1e-6, 0.39, 0.10 and 0.12 for **C-G**. Silencing of Orco ORNs and Gr5a GRNs reduce odor-evoked PER. (**H**) Integrated PER duration in control (*UAS-Kir2.1*/+, n = 21) and Gr66a GRN silenced (Gr66a-Gal4>UAS-Kir2.1, n = 21) flies in a fed state. Silencing of Gr66a GRNs enhances odor-evoked PER in a fed state. Odor concentration was 10^{-1}. p = 0.002. (**I**) Integrated PER duration in control (n = 29) and Gr5a mutant (n = 29) flies. PER is severely reduced in mutant flies. p = 1.0e-5. (**J-L**) Integrated PER duration in control and Obp RNAi flies. Obp57d/e RNAi flies show reduced (n = 33 and 25 for control and RNAi), Obp49a RNAi flies show enhanced (n = 24 and 20 for control and RNAi), and Obp19b RNAi flies show similar level of PER (n = 24 and 21 for control and RNAi) as compared to their respective controls. p = 0.006, 0.005, and 0.24 for **J-L**. Scheirer–Ray–Hare test. Box plots indicate the median (gray line), mean (black dot), quartiles (box), and 5-95% range (bar).

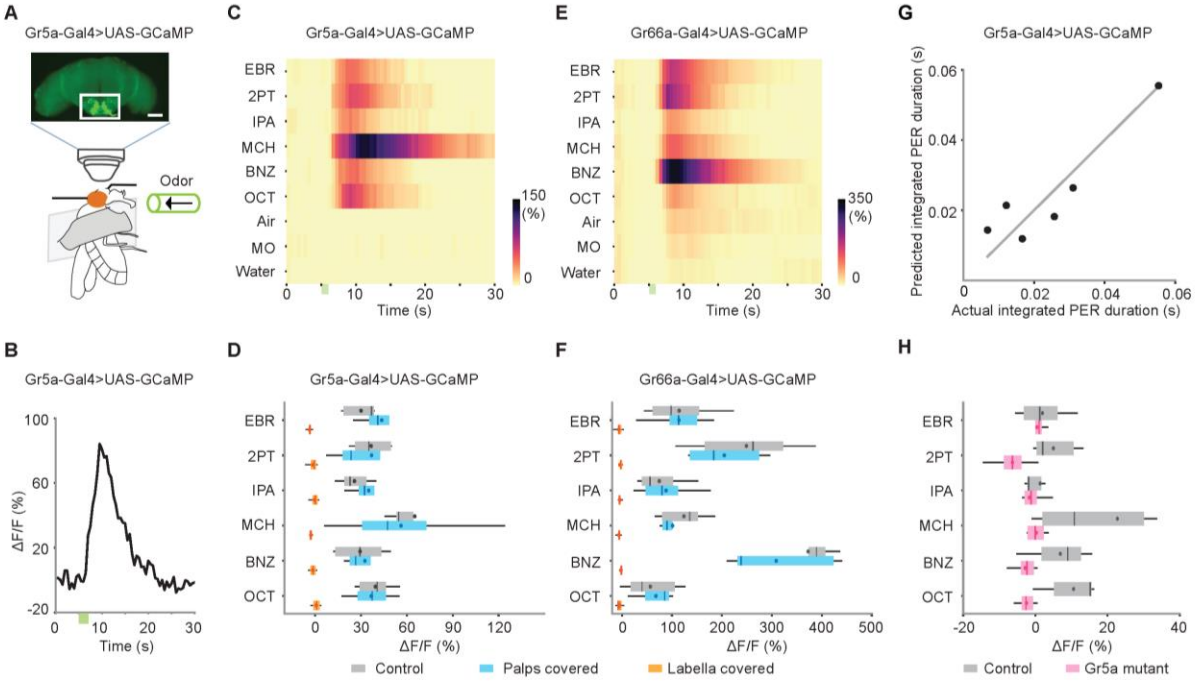

Figure 3. Sweet- and bitter-sensing GRNs directly respond to odors
(**A**) Schematic for two photon calcium imaging of GRN axon termini in the subesophageal zone. The top image shows an anterior view of a brain of Gr5a-Gal4>UAS-GCaMP6s fly. White rectangle indicates the target region of calcium imaging. Scale bar: 50 μm. (**B**) Example response (ΔF/F) to ethyl butyrate. Green bar indicates an odor application period. (**C**) Example responses of Gr5a GRNs to nine odors. Green bar indicates an odor application period. ΔF/F of GCaMP6s fluorescence is color coded according to the scale bar. (**D**) Trial averaged peak responses of Gr5a GRNs to individual odors. Covering the labella (n = 4, p = 2e-13) but not maxillary palps (n = 4, p = 0.15) with glue reduces odor responses as compared to control (n = 5). Two-way ANOVA. (**E**, **F**) Same as in **C**, **D**, but for Gr66a GRNs. As in Gr5a GRNs, covering the labella (n = 5, p = 9e-08) but not maxillary palps (n = 5, p = 0.56) with glue reduces odor responses as compared to control (n = 6). Two-way ANOVA. (**G**) A linear combination of Gr5a and Gr66a GRN responses well predicted the magnitude of odor-evoked PER. Each dot represents an odor. Coefficient of determination = 0.81. (**H**) Odor responses are severely reduced in Gr5a GRNs in a Gr5a receptor mutant background (n = 6 and 8 for control and mutant, p = 5e-06, two-way ANOVA). Box plots indicate the median (gray line), mean (black dot), quartiles (box), and 5-95% range (bar).

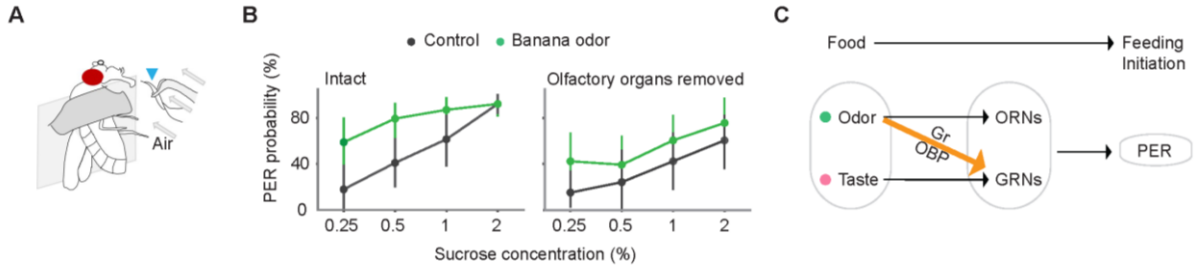

Figure 4. GRNs integrate odor-taste multisensory input to drive PER
(**A**) Schematic for examining PER in response to odor-taste multimodal stimuli. Stimuli are presented to the labellum with a wick (arrowhead) immersed in a sucrose solution with or without odors. A constant air stream was applied from behind the wick. (**B**) PER probability in response to sucrose at different concentrations with (green) or without (black) banana odor in wild type flies. Odor concentration was 10^{-4}. Banana odor enhances sucrose-evoked PER even in the absence of olfactory organs (n = 13 and 11, p = 0.002 and 0.04 for intact and olfactory organ removed flies). Scheirer–Ray–Hare test. Error bar, standard error of the mean. (**C**) Summary of mechanisms underlying PER in a multisensory environment.

Supplemental Figures

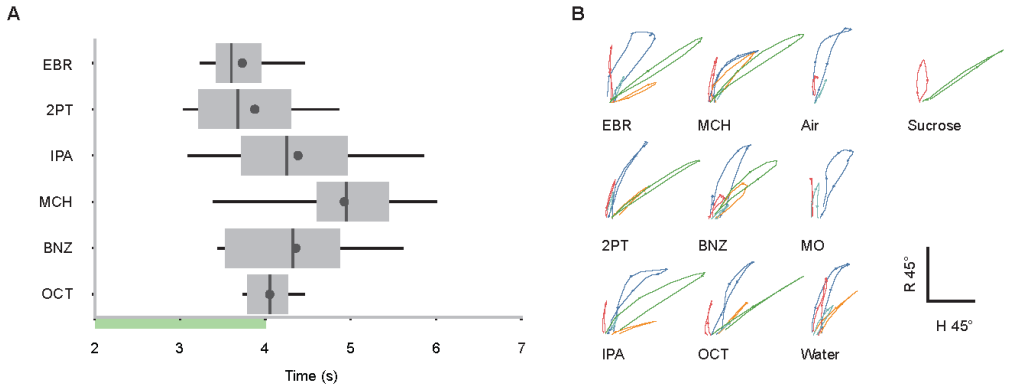

Figure S1. Characteristics of PER in wild type flies

(A) Latency to the first odor-evoked PER in wild type flies. Green bar indicates an odor application period. p = 1.0e-4, one-way ANOVA. Box plots indicate the median (gray line), mean (black dot), quartiles (box), and 5-95% range (bar). **(B)** K-medoid clustering of odor- and sucrose-evoked proboscis extensions based on the rostrum and haustellum angles over time in wild type flies. All the trajectories during PER and partial proboscis extensions were clustered into five clusters (color coded), and the representative trajectory closest to each cluster medoid was plotted for each stimulus. The green trajectories represent full extensions that qualify the definition of PER (see Methods). Note that these green trajectories are observed in response to sucrose and all the odors (except for the controls), suggesting that the movement of proboscis during odor-evoked PER is similar to that during sucrose-evoked PER.

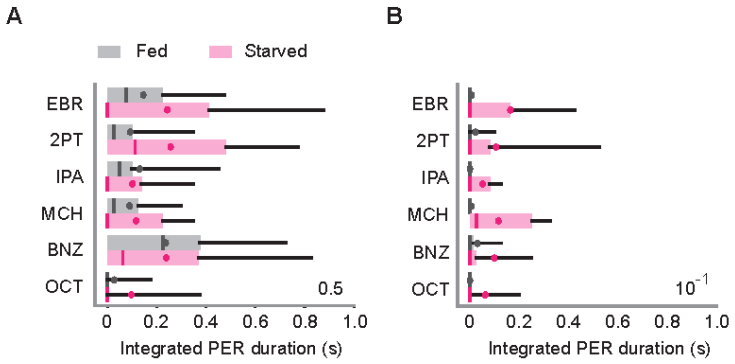

Figure S2. Dependence of odor-evoked PER on feeding state

(**A)** Integrated PER duration in starved (n = 28) and fed (n = 19) wild type flies. PER is enhanced in the starved state. p = 0.88, Scheirer–Ray–Hare test. (**B)** Same as in a but for odor concentration of 10^{-1}. p = 1e-6, Scheirer–Ray–Hare test. Box plots indicate the median (gray line), mean (black dot), quartiles (box), and 5-95% range (bar).

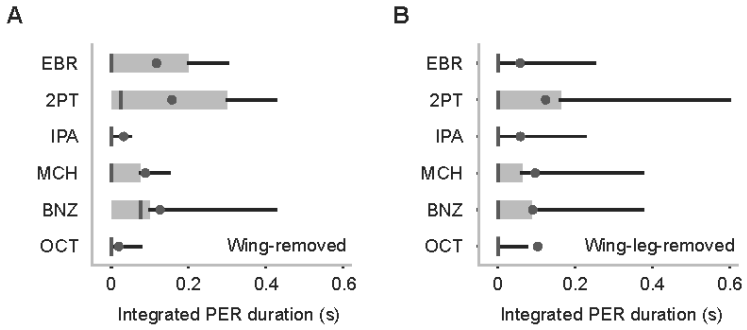

Figure S3. Wings and legs are not required for odor-evoked PER

(A) Integrated PER duration in wing-removed Orco-Gal4>UAS-Kir2.1 flies (n = 26). **(B)** Integrated PER duration in wing and leg-removed, Orco-Gal4>UAS-Kir2.1 flies (n = 27). These results suggest that GRNs in wings and legs are dispensable for odor-evoked PER. Box plots indicate the median (gray line), mean (black dot), quartiles (box), and 5-95% range (bar).

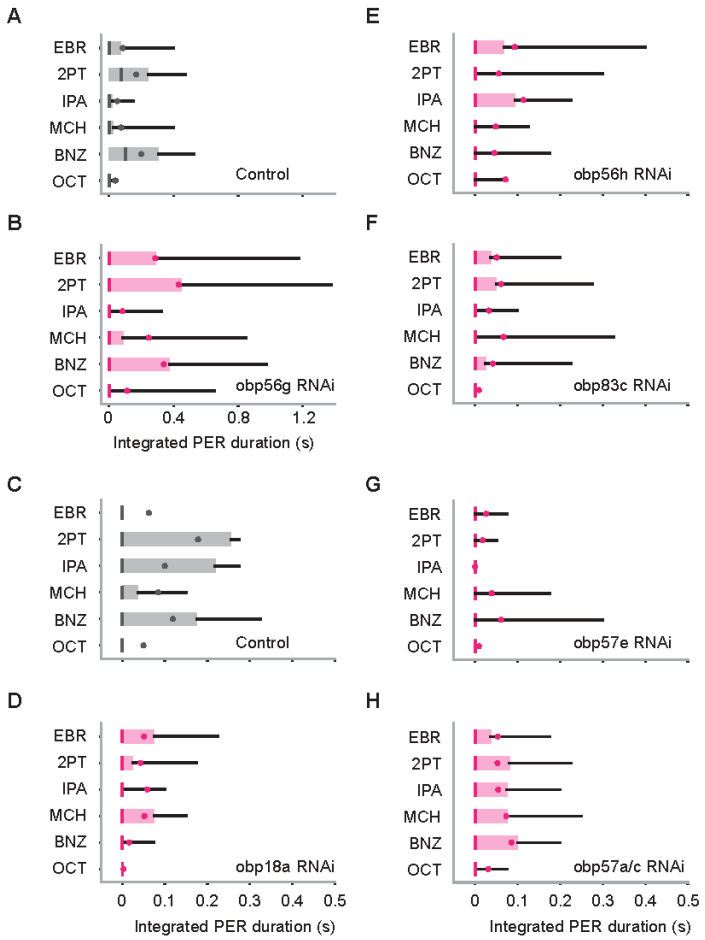

Figure S4. Contributions of OBPs to odor-evoked PER

(A, B) Integrated PER duration in control and Obp56g RNAi flies. These flies show similar level of PER (n = 24 and 23 for control and RNAi). p = 0.58, Scheirer–Ray–Hare test. (**C-H)** Integrated PER duration in control and OBP RNAi flies. Obp18a RNAi and Obp57e RNAi flies show reduced level of PER as compared to control. n = 33, 25, 22, 25, 27, and 28 flies for **C-H**. p = 0.05, 0.36, 0.08, 0.05, and 0.90 for **D-H**, Scheirer–Ray–Hare test. Box plots indicate the median (gray line), mean (black dot), quartiles (box), and 5-95% range (bar).

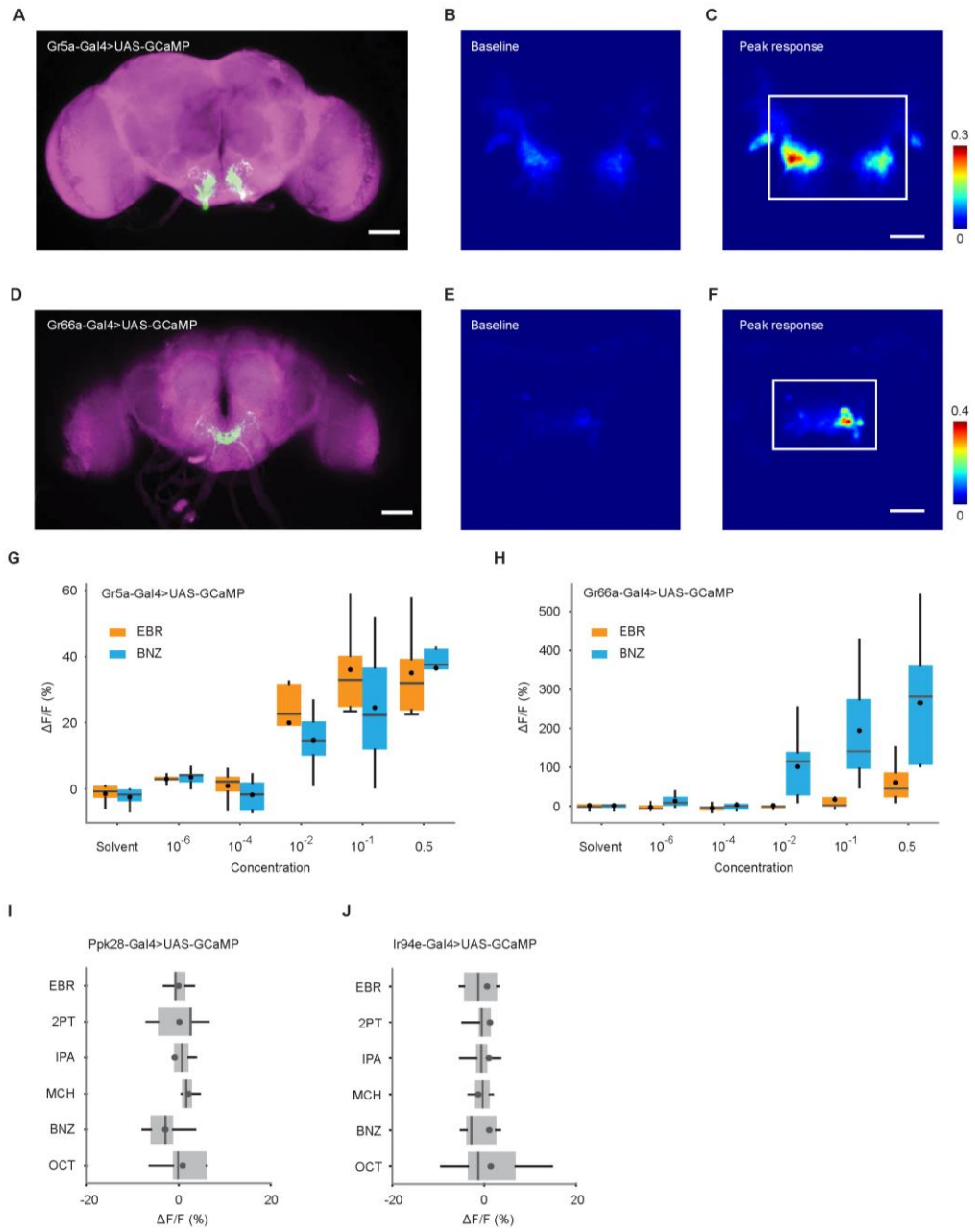

Figure S5. Responses of GRNs to odors and sucrose

(A) Image of a brain of Gr5a-Gal4>UAS-GCaMP6s fly, stained with anti-GFP to reveal Gr5a neurons (green) and nc82 to reveal synapses (magenta). Scale bar, 50 µm. (**B)** Baseline florescence intensity of GCaMP6s in Gr5a GRNs. Fluorescence (arbitrary unit) is color coded according to the scale bar. **(C)** Peak florescence intensity of GCaMP6s in the same fly as shown in B after stimulation with 4-methylcyclohexanol. Fluorescence is color coded according to the scale bar. The ROI used for ΔF/F calculation is indicated by a white rectangle. Scale bar, 20 µm. (**D-F)** Same as in **A-C**, but for Gr66a-Gal4>UAS-GCaMP6s fly and benzaldehyde stimulation. (**G)** Trial averaged peak responses of Gr5a GRNs to different concentrations of ethyl butyrate (EBR) and benzaldehyde (BNZ). n = 5 flies. (**H)** Same as in **G,** but for Gr66a GRNs. (**I)** Trial

averaged peak responses of Ppk28 GRNs to individual odors. These neurons do not respond to odors. n = 5 flies. (**J)** Same as in **I**, but for Ir94e GRNs. n = 9 flies. Box plots indicate the median (gray line), mean (black dot), quartiles (box), and 5-95% range (bar).

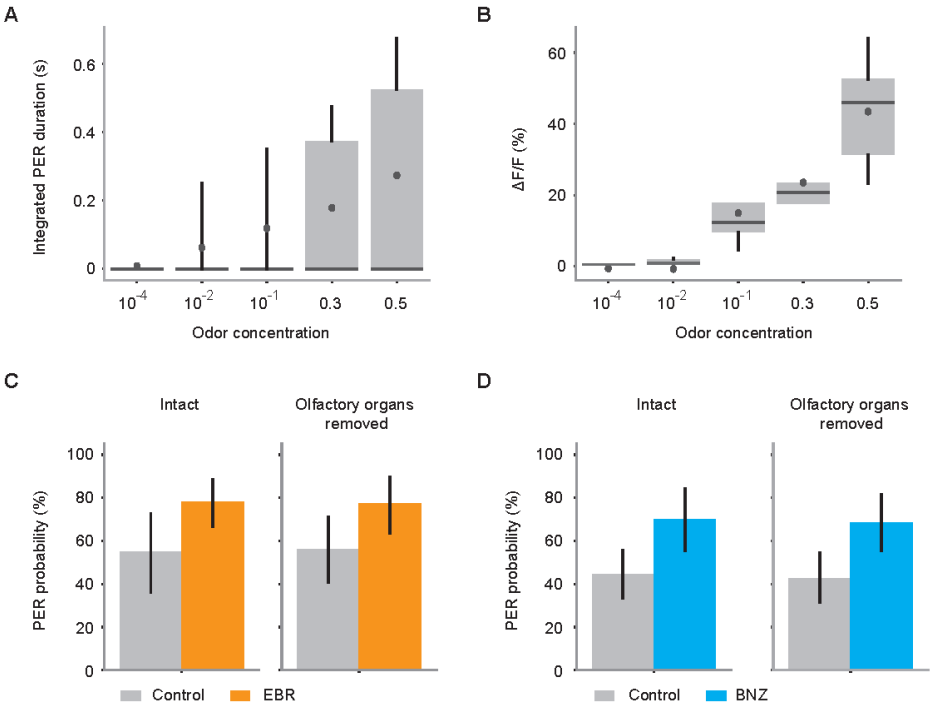

Figure S6. Multisensory PER in flies with intact or removed olfactory organs

(A) Integrated PER duration in response to a banana odor presented at various concentrations in wild type flies. n = 21 flies. Box plots indicate the median (gray line), mean (black dot), quartiles (box), and 5-95% range (bar). (**B)** Trial averaged peak responses of Gr5a GRNs in response to various concentrations of banana odor in Gr5a-Gal4>UAS-GCaMP6s flies. n = 5 flies. (**C)** PER probability in response to sucrose with or without odors in wild type flies in which olfactory organs are intact or have been removed. Odor is EBR. Intact, n = 25, p = 0.005. Olfactory organs removed, n = 25, p = 0.007. Wilcoxon signed-rank test. (**D)** Same as in **C**, but for BNZ. Intact, n = 21, p = 0.007. Olfactory organs removed, n = 36, p = 0.0007. Wilcoxon signed-rank test.

The concentration of odors and sucrose was 10^{-4} and 0.25%, respectively. Error bar, standard error of the mean.

Movie S1. Odor-evoked PER

A video capturing odor-evoked PER associated with the plot of haustellum angle over time. Six points on the head were tracked by DeepLabCut.